Published in final edited form as:
J Am Chem Soc. 2013 April 3; 135(13): 4978–4981. doi:10.1021/ja401612x.

Passive Tumor Targeting of Renal Clearable Luminescent Gold Nanoparticles: Long Tumor Retention and Fast Normal Tissue Clearance

Jinbin Liu, **Mengxiao Yu**, **Chen Zhou**, **Shengyang Yang**, **Xuhui Ning**, and **Jie Zheng***
Department of Chemistry, The University of Texas at Dallas, Richardson, Texas 75080, United States

Abstract

Glutathione-coated luminescent gold nanoparticles (GS-AuNPs) of ~ 2.5 nm behave like small dye molecules (IRdye 800CW) in physiological stability and renal clearance, but exhibit much longer tumor retention time and faster normal tissue clearance than the dye molecules, indicating that well-known enhanced permeability and retention (EPR) effect, a unique strength of conventional nanoparticles (NPs) in tumor targeting, still exists in such small NPs. These merits enable the AuNPs to more rapidly detect tumor than the dye molecules without severe accumulation in reticuloendothelial system (RES) organs, holding great promise in cancer diagnosis and therapy.

Inorganic nanoparticles (NPs) with large surface areas, tunable material properties and strong signal output[1] potentially serve as a new generation of nanomedicines, which can catalyze the shift of our current medical paradigm to “earlier detection and prevention”.[2] NPs often passively accumulate in the disease sites such as tumors at much higher concentrations and longer time than small drug molecules through a well-known enhanced permeability and retention (EPR) effect,[3] making NPs even more promising in addressing many challenges that small drug molecules encounter in early cancer diagnosis and therapy.[2a] For example, 30 nm gold nanocages coated with PEG molecules can passively target tumors with a high efficiency of 8 % injected dose per gram (% ID/g) of tissue after 24 hr post injection (p.i.).[4] This unique strength of NPs in tumor targeting is fundamentally because NPs can escape kidney filtration and retain in the blood plasma for longer time than small molecules do.[3b] However, unlike small renal clearable clinically used molecular probes such as 2-deoxy-2-[18F]fluoro-D-glucose ([18F] FDG),[5] Gd-DTPA,[6] and iomeprol,[7] inorganic NPs often severely accumulate in reticuloendothelial system (RES) organs (liver and spleen etc.),[8] resulting in low targeting specificity (defined as the amount of probes in tumor versus that in liver)[9] and potential long-term toxicity,[10] hampering their future clinical applications.

*Corresponding Author: jiezheng@utdallas.edu.

Supporting Information

Experimental procedures, calculations of contrast index and retention kinetics in normal tissue and tumor, characterizations of the GS-AuNP and IRdye 800CW, stability studies, additional in vivo NIR fluorescence images, additional time dependence contrast indexes, additional retention kinetics, additional tumor targeting kinetics, standard curve of IRdye 800CW, TEM and DLS characterization of BSA-AuNPs, and Tables S1-S2. This material is available free of charge via the Internet at http://pubs.acs.org.

To minimize nonspecific accumulation in RES organs and potential toxicity of inorganic NPs, several different kinds of renal clearable inorganic NPs have been developed recently.[11] For instance, Choi et al.[12] found that cysteine coated quantum dots (QDs) (CdSe/ZnS) with hydrodynamic diameter (HD) below 5.5 nm can be efficiently cleared out into the urine within 4 hr and less than 10 % of the QDs accumulated in the RES organs. Our recent studies[13] showed that glutathione (GSH), a small tri-peptide, can serve as an effective surface ligand to minimize non-specific RES uptake of few-nm luminescent gold NPs (GS-AuNPs) and enabled more than 60 % of the particles to be cleared out through the urinary system and only 3 % ID/g of the NPs were found in the liver after 48 hr of p.i..[13c] More detailed pharmacokinetics studies[13b] reveal that GS-AuNPs rapidly distribute in the body with a fast distribution half-life of 5.0 min and circulate in the body with a long blood elimination half-life of 12.7 hr in balb/c mice.

While these renal clearable inorganic NPs behave like small molecules in urinary elimination and two-compartment pharma-cokinetics due to their small size and desired surface chemistry, whether renal clearable NPs will retain EPR effect, a unique strength of conventional NPs in passive tumor targeting, is unknown but critical to their future applications in disease diagnosis and therapy. For the EPR effect to function well, NPs often need to remain in the blood plasma at a relatively high concentration for more than 6 hr.[3b] Thus, macromolecules or NPs with sizes larger than 40 kDa or 5.5 nm that can escape kidney filtration generally exhibit desired EPR effect.[3b,12a] However, to evade RES uptake, NPs need to be smaller than the kidney filtration threshold (5.5 nm).[12a] Therefore, these seemingly contradictory requirements on NP size naturally raise a fundamental question of whether renal clearable NPs with HD smaller than kidney filtration threshold can still have prolonged retention time in the tumor as their large counterparts. In addition, since imaging contrast index (CI), a parameter to report the quality of imaging detection, is dependent on the ratio of the amount of probe in tumor to that in normal tissue background, the clearance of the probes from normal tissues also plays a key role in contrast enhancement and rapid detection.[14] However, how renal clearable NPs are eliminated from the normal tissues in comparison with renal clearable small molecules has not been investigated before.

With these two fundamental questions, we conducted a detailed comparison on passive tumor targeting of a renal clearable near-infrared (NIR) emitting inorganic NP, GS-AuNP, and a renal clearable organic fluorophore, IRdye 800CW[15] (Figure 1). The synthesis procedures of the 2.5 nm NIR emitting GS-AuNPs were reported before,[13b,16] and the modified synthesis procedures along with necessary characterizations such as elemental analysis, TEM, fluorescence spectra, FT-IR spectra, and DLS measurements were described in the supporting information (Figures S1–S3) for future reference. These two probes have comparable emission wavelengths (~ 800 nm) and high physiological and photostability suitable for real-time imaging of passive tumor targeting and retention kinetics in tumor and normal tissues (Figure S4). Our findings show that while GS-AuNPs and IRdye 800CW behave similarly in initial tumor targeting, they exhibit distinct retention kinetics in tumor and normal tissues: GS-AuNPs retained in the tumor at a concentration 10 times higher than the dye molecules after 12 hr p.i. but GS-AuNPs were cleared out from the normal tissues more than 3 times faster than the dye molecules. As a result, the contrast index of the NPs reached the detection threshold (2.5) nearly 3 times faster than the dye molecule. These

results clearly indicate that renal clearable GS-AuNPs with HD (3.3 nm) smaller than the kidney filtration threshold (5.5 nm) indeed can passively target tumor through EPR effect and they are more suitable for rapid tumor detection than organic dye molecules. These new findings on passive tumor targeting of renal clearable AuNPs, distinct from small dye molecules and conventional non-renal clearable NPs, are expected to further guide chemists to design a new generation of nanomedicines for clinical practices.

Passive tumor targeting of GS-AuNPs and IRdye 800CW was investigated by collecting in-situ fluorescence images of MCF-7 tumor-bearing nude mice at different p.i. time points (Figure 2A). While the mice were barely imaged in NIR region before the injection of the probes, they became visible right after the IV injection of the probes due to the rapid distribution of the probes in the mice. However, tumor areas were hardly defined in the mice in the first 0.5 hr p.i. because of strong fluorescence background from the probes in normal tissue (Figure 2A). With the time increasing, the decrease of fluorescence background from normal tissues made the tumor areas to be readily defined in the mouse injected with GS-AuNPs at 3 hr p.i. (Figure 2A), but not in the one with dye molecules, which required additional 5 hr to obtain clear tumor images (Figure S5). At 12 hr p.i., the tumor area in the mouse injected with GS-AuNPs became more evident due to the well maintained signal from the tumor site and the further decrease of fluorescence background from normal tissues. In contrast, significant decrease in emission from the tumor in the mouse with the dye indicated that most dye molecules were eliminated from tumors after 12 hr p.i. (Figures 2A and S5). Besides the tumor, the bladder is another major organ, where the accumulation and elimination of both probes are readily observed (Figure 2A), which confirmed the renal clearance of the particle and the dye, consistent with the previous observations of luminescent GS-AuNPs,[13b,13c] and IRdye 800CW.[15]

Ex vivo images of the organs and tumors taken from the mice injected with the probes show that the tumors from the mice injected with GS-AuNPs exhibit comparable signals at 1 and 12 hr p.i. (Figure 2B) while the emission signal from the tumor of the mouse with the dye at 12 hr p.i. was significantly lower than the one at 1 hr p.i. (Figure 2C), further confirming that GS-AuNPs indeed have much longer retention time in the tumor than the dye molecules. However, emission intensities of both probes in the kidney at 12 hr p.i. were significantly lower than those at 1 hr p.i. (Figures 2B and 2C), indicating that both probes were cleared out the body through kidney filtration. Consistence in the accumulation of the probes in the tumor and kidney between in vivo and ex vivo studies clearly indicates that it is feasible to noninvasively image tumor targeting and renal clearance of both probes at the in vivo level in real time.

As contrast index (CI) is a general parameter used in tumor imaging to evaluate how well the tumor could be distinguished from normal tissues due to the introduction of probes,[17] we quantified the time-dependent CI values of GS-AuNPs and IRdye 800CW. Generally, CI value at 2.5 is considered to be a threshold for a substantial tumor targeting.[18] Shown in Figures 3A and S6, and Table S1 that it took 3.1 ± 0.2 hr and 8.2 ± 0.6 hr for the NPs and the dye molecules to reach a CI value of 2.5, respectively. While CI value of GS-AuNPs (~ 3.0) is slightly lower than that of the reported renal clearable quantum dots (QDs) conjugated with active tumor targeting ligands (5.0), it is higher than that of renal clearable

QDs without active targeting ligands (1.8).[12b] Differences in CI kinetics between the NPs and the dye fundamentally arise from distinctive retention kinetics of both probes in normal tissues and tumors. As shown in Figures 3B and S7, fluorescence intensitiy of normal tissues of the mice injected with the IRdye 800CW reached its maximum after 40 ~ 50 min p.i., but it only took less than 10 min for GS-AuNP to reach its maximum (Figure 3B and Table S2). The retention kinetics of the IRdye 800CW in the normal tissues exhibited a monoexponential decay with a half-life of 2.3 ± 0.3 hr (Figure 3B). In contrast, retention kinetics of the GS-AuNPs in normal tissue showed two-compartment decay: more than 90 % of the NPs were eliminated from the normal tissues with a half-life of 43.4 ± 6.6 min and less than ~ 10 % of the NPs remained in the normal tissue for more than 24 hr. These results indicated that the majority of the NPs were cleared out from the normal tissue more than 3 times faster than the dye molecules.

Subsequent analysis of time-dependent emission intensities from tumor also revealed some similarities and differences in the tumor targeting between the NPs and dye molecules (Figures 3C and S8). Both probes reached their maximum accumulation at the tumor sites within 40 min, indicating that the NP behaved like the small dye molecule in the initial stage of the tumor targeting. However, the retention kinetics of the NP and dye molecule in tumor was different. For IRdye 800CW, it followed a biexponen-tial decay with half-lives of 1.4 ± 0.6 hr (70.7 ± 9.2 %) and 6.2 ± 0.3 hr (29.3 ± 9.2 %). While the origin of these two-compartment decay is still not clear, we hypothesize that the observed shorter half-life (~ 1.4 hr) might result from the dense blood vessels in tumors, making the dye molecules more easily diffuse away from the tumors than the normal tissues (2.3 ± 0.3 hr). However, the longer half-life (6.2 ± 0.3 hr) might be due to the leakiness of the tumor vascular structure and the trap of the dye molecules inside the tumors. Less than 5 % of the maximum fluorescence intensity remained in the tumor site after 24 hr of p.i., indicating that the dye molecules can be eventually cleared out of the tumors. In sharp contrast, more than 76 % of the maximum fluorescence intensity from the NPs remained in the tumor after 24 hr of p.i., which implies that the tumor retention of GS-AuNPs is much longer than that of IRdye 800CW. Such distinct tumor retention behaviour between GS-AuNPs and IRdye 800 CW suggest that EPR effect do exist in GS-AuNPs even though HD (3.3 nm) of GS-AuNPs is smaller than kidney filtration size (5.5 nm).

We then compared the pharmacokinetics of both GS-AuNPs and IRdye 800CW in nude mice to further understand the origin of EPR effect. While the particles and dye molecule are both renal clearable, their pharmacokinetics are not exactly the same. As shown in Figure 4D, both two probes followed two-compartment pharmacokinetics. GS-AuNPs and IRdye 800CW exhibited comparable distribution half-lives ($t_{1/2\alpha}$), which were 5.4 ± 1.2 and 6.3 ± 2.5 min, respectively. The very short $t_{1/2\alpha}$ is a typical characteristic of many small molecular probes. For example, the $t_{1/2\alpha}$ of Gd-DTPA and iomeprol are 0.4 and 16.2 min,[6–7] respectively. Since the distribution half-life reflects how fast a probe distributes in the body, very short half-life of the particles indicated that the renal clearable GS-AuNPs indeed behave more like small molecules rather than conventional large NPs in the initial tissue distribution,[13b] which was consistent with their initial tumor targeting. However, the blood elimination half-life $t_{1/2\beta}$ of the GS-AuNP in nude mice was 8.5 ± 2.1 hr, which is slight shorter than 12.7 hr observed in balb/c mice[13b] but nearly one-order longer than that of the

dye (0.98 ± 0.08 hr). Such long blood elimination half-life is responsible for the origin of EPR effect in renal clearable GS-AuNPs, which meets the minimum requirement (6 hr) for strong EPR effect.[3b] The $t_{1/2\beta}$ of GS-AuNP (8.5 hr) is 4 times longer than that of 5.5 nm renal clearable cysteine coated QDs (~ 2 hr),[12] which is also the reason why the CI value of GS-AuNPs (~ 3.0) is higher than that of renal clearable QDs without active targeting ligands (1.8).[12b]

To gain more quantitative understandings of in vivo behaviors of both probes, we studied the biodistribution of the NPs and dye molecules at 1 and 12 hr, respectively (Figures 4A and 4B). The tumor uptakes were measured to be 3.0 ± 0.2 and 2.3 ± 0.2 % ID/g for the GS-AuNPs, and 1.8 ± 0.1 and 0.2 ± 0.02 % ID/g for the IRdye 800 CW at 1 and 12 hr, respectively. These data demonstrated that GS-AuNPs indeed retained in the tumor much longer than IRdye 800CW and at a concentration 10 times higher than that of the dye molecules at 12 hr p.i., consistent well with the in vivo kinetics results (Figures 2 and 3A-3C). This prolonged tumor retention behaviour is very similar to those of the reported large PEG coated AuNPs (PEG-AuNPs) with sizes ranging from 20 to 100 nm, which also exhibit long retention in tumor due to EPR effect.[19] The reason for observing EPR effect in GS-AuNPs is because GSH behaves like the PEG molecule in resistance to serum protein adsorption, which allows GS-AuNPs to retain in the blood plasma at a relatively highly concentration like those 20 ~ 100 nm PEG-AuNPs[19] in tumor targeting. However, it should be noted that GS-AuNPs do exhibit some differences in some passive tumor targeting behaviours compared to those nonrenal clearable PEG-AuNPs.[19] In terms of tumor accumulation kinetics, GS-AuNPs reached its highest accumulation within 1 hr, much faster than those large PEG-AuNPs,[19] which generally reach their maxima after 4 ~ 8 hr p.i. and the targeting efficacy of GS-AuNPs is generally 2 ~ 10 times better than those of 20 ~ 100 nm PEG-AuNPs.[19] Another advantage of renal clearable AuNPs over non-renal clearable ones is that targeting specificity of GS-AuNPs is much higher than those nonrenal clearable AuNPs. As control, we investigated tumor targeting specificity of ~ 30 nm bovine serum albumin (BSA) coated AuNPs (BSA-AuNPs) (HD: ~ 60 nm, Figure S10) under the same conditions and found that more than 70 % ID were rapidly shuttled out of circulation to the liver and spleen (Figure 4C). As a result, tumor targeting specificities of 30 nm BSA-AuNPs were only 0.0036 ± 0.0007 and 0.0030 ± 0.001 at 1 hr and 12 hr, respectively, which were more than 300 times less than those of GS-AuNPs and the dye at both 1 hr and 12 hr p.i. (Figure 4D). Generally, the targeting specificity of GS-AuNPs is one or two orders better than those of nonrenal clearable AuNPs because accumulation of GS-AuNPs in RES is more than 10 times lower than those of large AuNPs (30 % ~ 60 % ID/g).[4,19–20]

In summary, we systematically compared in vivo passive tumor targeting of a renal clearable AuNP and a dye molecule. While the renal clearable NPs behave like small renal clearable molecules in the initial stage of tumor targeting, the tumor retention time of the NPs is much longer than that of dye molecule, indicating that GS-AuNPs do retain EPR effect while achieving efficient renal clearance. The origin of EPR effect in renal clearable luminescent AuNPs is likely because GS-AuNPs evade the uptake of the RES organs and retain in the blood plasma with a relatively long elimination half-life of 8.5 hr. In addition, clearance of GS-AuNPs from normal tissues is more than 3 times faster than the dye molecules; as a result, the contrast index of the NPs increases more rapidly than that of the

small dye molecules (3 hr vs 8 hr), implying that renal clearable luminescent AuNPs are more suitable for rapid detection of tumors than small dye molecules. With rapid clearance in normal tissues, long retention in tumors and high tumor targeting specificity, these renal clearable luminescent AuNPs circumvent the dilemma in the requirements for EPR effect and minimization of RES uptake, holding great promise in the translation of inorganic nanomedicines into the clinical practices.

Supplementary Material

Refer to Web version on PubMed Central for supplementary material.

Acknowledgments

This work was supported in part by the NIH (R21EB009853 and 1R21EB011762), CPRIT (RP120588) and the start-up fund from the University of Texas at Dallas (J.Z.). We would like to thank Dr. Li Liu at The University of Texas Southwestern Medical Center for teaching tumor implantation.

References

1. (a) Qian H, Eckenhoff WT, Zhu Y, Pintauer T, Jin R. J Am Chem Soc. 2010; 132:8280. [PubMed: 20515047] (b) Liu YD, Han XG, He L, Yin YD. Angew Chem Int Edit. 2012; 51:6373.(c) Zrazhevskiy P, Sena M, Gao XH. Chem Soc Rev. 2010; 39:4326. [PubMed: 20697629]
2. (a) Ferrari M. Nat Rev Cancer. 2005; 5:161. [PubMed: 15738981] (b) Huang XH, Peng XH, Wang YQ, Wang YX, Shin DM, El-Sayed MA, Nie SM. Acs Nano. 2010; 4:5887. [PubMed: 20863096] (c) Xing H, Wong NY, Xiang Y, Lu Y. Curr Opin Chem Biol. 2012; 16:429. [PubMed: 22541663] (d) Zhou M, Zhang R, Huang M, Lu W, Song S, Melancon MP, Tian M, Liang D, Li C. J Am Chem Soc. 2010; 132:15351. [PubMed: 20942456] (e) Cheng Y, ACS, Meyers JD, Panagopoulos I, Fei B, Burda C. J Am Chem Soc. 2008; 130:10643. [PubMed: 18642918] (f) Chou SW, Shau YH, Wu PC, Yang YS, Shieh DB, Chen CC. J Am Chem Soc. 2010; 132:13270. [PubMed: 20572667] (g) Lee H, Yu MK, Park S, Moon S, Min JJ, Jeong YY, Kang HW, Jon S. J Am Chem Soc. 2007; 129:12739. [PubMed: 17892287] (h) Robinson JT, Hong G, Liang Y, Zhang B, Yaghi OK, Dai H. J Am Chem Soc. 2012; 134:10664. [PubMed: 22667448] (i) Lee JE, Lee N, Kim H, Kim J, Choi SH, Kim JH, Kim T, Song IC, Park SP, Moon WK, Hyeon T. J Am Chem Soc. 2010; 132:552. [PubMed: 20017538] (j) Ling D, Park W, Park YI, Lee N, Li F, Song C, Yang SG, Choi SH, Na K, Hyeon T. Angew Chem Int Edit. 2011; 50:11360.
3. (a) Matsumura Y, Maeda H. Cancer Res. 1986; 46:6387. [PubMed: 2946403] (b) Iyer AK, Khaled G, Fang J, Maeda H. Drug Discov Today. 2006; 11:812. [PubMed: 16935749]
4. Wang Y, Liu Y, Luehmann H, Xia X, Brown P, Jarreau C, Welch M, Xia Y. Acs Nano. 2012; 6:5880. [PubMed: 22690722]
5. Liu RS, Chou TK, Chang CH, Wu CY, Chang CW, Chang TJ, Wang SJ, Lin WJ, Wang HE. Nucl Med Biol. 2009; 36:305. [PubMed: 19324276]
6. Kobayashi H, Sato N, Hiraga A, Saga T, Nakamoto Y, Ueda H, Konishi J, Togashi K, Brechbiel MW. Magnet Reson Med. 2001; 45:454.
7. Lorusso V, Taroni P, Alvino S, Spinazzi A. Invest Radiol. 2001; 36:309. [PubMed: 11410750]
8. Zamboni WC. Clin Cancer Res. 2005; 11:8230. [PubMed: 16322279]
9. (a) Dobrovolskaia MA, McNeil SE. Nat Nanotechnol. 2007; 2:469. [PubMed: 18654343] (b) Kareem H, Sandstrom K, Elia R, Gedda L, Anniko M, Lundqvist H, Nestor M. Tumour Biol. 2010; 31:79. [PubMed: 20358420]
10. Yang RH, Chang LW, Wu JP, Tsai MH, Wang HJ, Kuo YC, Yeh TK, Yang CS, Lin P. Environ Health Persp. 2007; 115:1339.
11. (a) Park JH, Gu L, von Maltzahn G, Ruoslahti E, Bhatia SN, Sailor MJ. Nat Mater. 2009; 8:331. [PubMed: 19234444] (b) Choi HS, Ipe BI, Misra P, Lee JH, Bawendi MG, Frangioni JV. Nano Lett. 2009; 9:2354. [PubMed: 19422261] (c) Gao J, Chen K, Xie R, Xie J, Lee S, Cheng Z, Peng

X, Chen X. Small. 2010; 6:256. [PubMed: 19911392] (d) Lux F, Mignot A, Mowat P, Louis C, Dufort S, Bernhard C, Denat F, Boschetti F, Brunet C, Antoine R, Dugourd P, Laurent S, Vander Elst L, Muller R, Sancey L, Josserand V, Coll JL, Stupar V, Barbier E, Remy C, Broisat A, Ghezzi C, Le Duc G, Roux S, Perriat P, Tillement O. Angew Chem Int Edit. 2011; 50:12299.

12. (a) Choi HS, Liu W, Misra P, Tanaka E, Zimmer JP, Ipe BI, Bawendi MG, Frangioni JV. Nat Biotechnol. 2007; 25:1165. [PubMed: 17891134] (b) Choi HS, Liu WH, Liu FB, Nasr K, Misra P, Bawendi MG, Frangioni JV. Nat Nanotechnol. 2010; 5:42. [PubMed: 19893516]
13. (a) Yu MX, Zhou C, Liu JB, Hankins JD, Zheng J. J Am Chem Soc. 2011; 133:11014. [PubMed: 21714577] (b) Zhou C, Hao GY, Thomas P, Liu JB, Yu MX, Sun SS, Oz OK, Sun XK, Zheng J. Angew Chem Int Edit. 2012; 51:10118.(c) Zhou C, Long M, Qin Y, Sun X, Zheng J. Angew Chem Int Edit. 2011; 50:3168.(d) Zhou C, Sun C, Yu MX, Qin YP, Wang JG, Kim M, Zheng J. J Phys Chem C. 2010; 114:7727.(e) Zheng J, Zhou C, Yu MY, Liu JB. Nanoscale. 2012; 4:4073. [PubMed: 22706895]
14. Kobayashi H, Longmire MR, Ogawa M, Choyke PL. Chem Soc Rev. 2011; 40:4626. [PubMed: 21607237]
15. Marshall MV, Draney D, Sevick-Muraca EM, Olive DM. Mol Imaging Biol. 2010; 12:583. [PubMed: 20376568]
16. Tu X, Chen W, Guo X. Nanotechnology. 2011; 22:095701. [PubMed: 21258146]
17. Jiang T, Olson ES, Nguyen QT, Roy M, Jennings PA, Tsien RY. Proc Natl Acad Sci USA. 2004; 101:17867. [PubMed: 15601762]
18. (a) Andreev OA, Dupuy AD, Segala M, Sandugu S, Serra DA, Chichester CO, Engelman DM, Reshetnyak YK. Proc Natl Acad Sci USA. 2007; 104:7893. [PubMed: 17483464] (b) Zhang EL, Zhang C, Su YP, Cheng TM, Shi CM. Drug Discov Today. 2011; 16:140. [PubMed: 21182981]
19. Perrault SD, Walkey C, Jennings T, Fischer HC, Chan WCW. Nano Lett. 2009; 9:1909. [PubMed: 19344179]
20. (a) Puvanakrishnan P, Park J, Chatterjee D, Krishnan S, Tunnell JW. Int J Nanomedicine. 2012; 7:1251. [PubMed: 22419872] (b) Zhang G, Yang Z, Lu W, Zhang R, Huang Q, Tian M, Li L, Liang D, Li C. Biomaterials. 2009; 30:1928. [PubMed: 19131103]

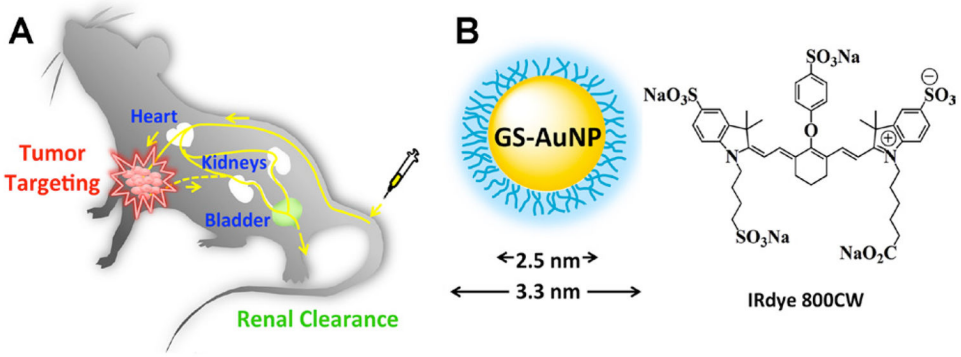

Figure 1.

Passive tumor targeting of renal clearable probes. A) The scheme of passive tumor targeting of renal clearable probes. In vivo tumor targeting and clearance kinetics can be measured by fluorescence imaging in real time after intravenous (IV) injection of the probes into nude mice. B) Schematic representation of the structures of glutathione coated NIR emitting gold nanoparticle (GS-AuNP; core size: 2.5 nm; hydrodynamic diameter: 3.3 nm) and the chemical structure of IRdye 800CW.

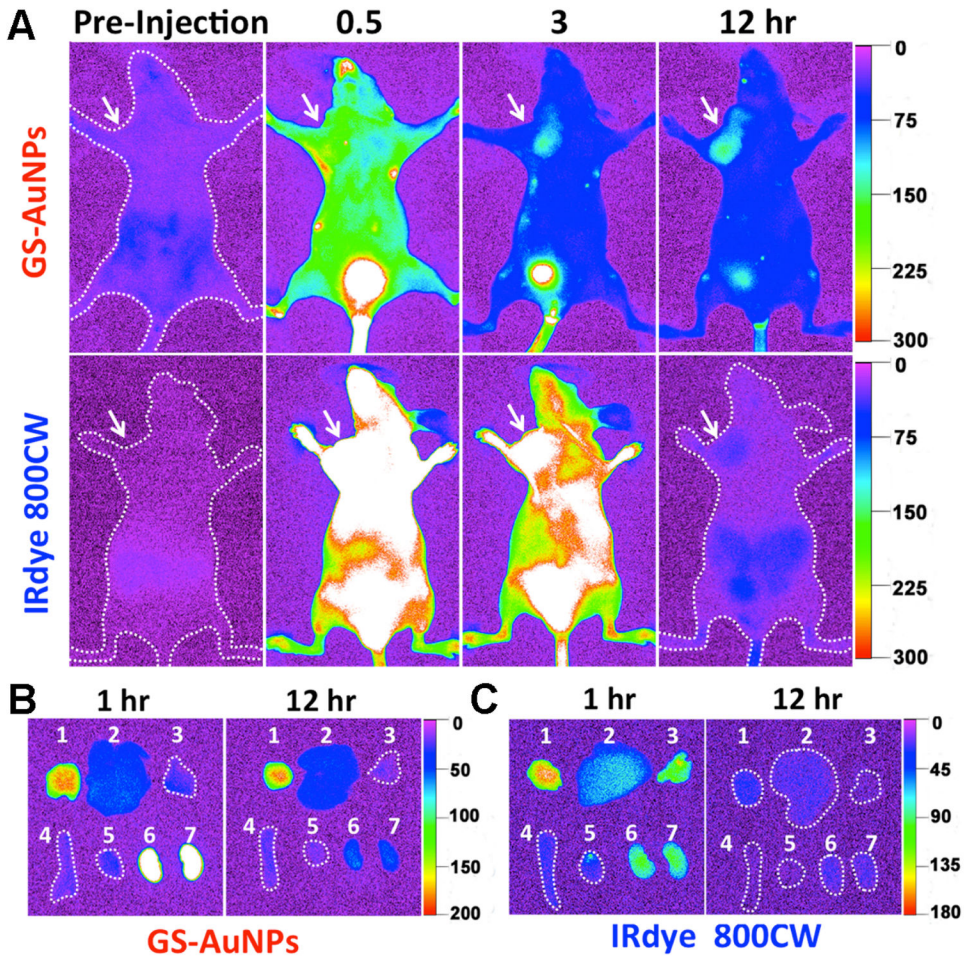

Figure 2.

In vivo and ex vivo NIR fluorescence imaging of MCF-7 tumor-bearing mice IV injected with GS-AuNPs and IRdye 800CW. A) Representative in vivo NIR fluorescence images collected at p.i. time points of 0.5, 3, and 12 hr, respectively. The tumor areas were indicated with arrows. B, C) Ex vivo fluorescence images of organs and tumors taken from the MCF-7 tumor-bearing mice IV injected with GS-AuNPs (B) and IRdye 800CW (C) at the time points of 1 and 12 hr p.i., respectively. In each image: 1, tumor; 2, liver; 3, lung; 4, spleen; 5, heat; 6, kidney (left); 7, kidney (right). More images related to the tumor targeting of the IRdye 800CW were shown in Figure S5.

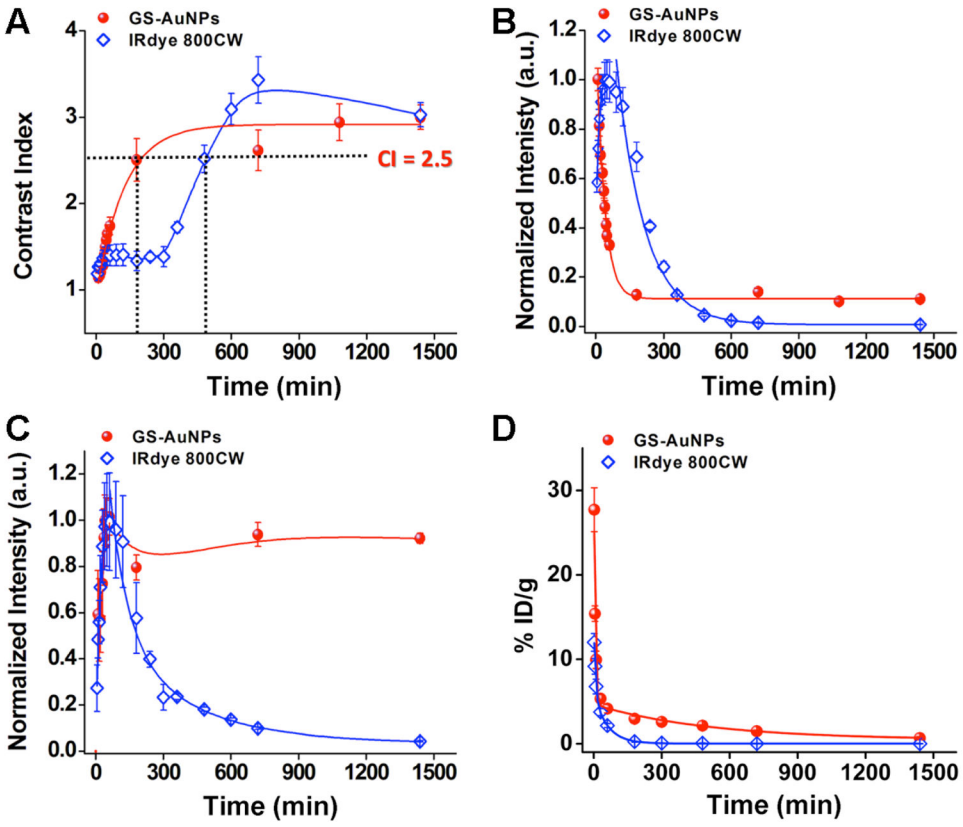

Figure 3.

Quantitative analysis of passive tumor targeting of GS-AuNPs and IRdye 800CW. A) Contrast index (CI) of GS-AuNPs and IRdye 800CW at different p.i. time points showing that the NP reach the maximum CI value faster than the dye molecule. To reach the CI threshold value (CI = 2.5) for a potential imaging probe, it took 3.1 ± 0.2 and 8.2 ± 0.6 hr for the NP and the dye molecule, respectively. B) Retention kinetics in normal tissue showing the retention half-lives of GS-AuNPs and IRdye 800CW are 43.4 ± 6.6 min and 2.3 ± 0.3 hr (n = 3), respectively. C) Tumor targeting kinetics of GS-AuNPs and IRdye 800CW, respectively. D) Pharmacokinetics of the renal clearable GS-AuNP and IRdye 800CW after the IV injection in 24 hr, respectively. The curves of pharmacokinetics were fitted to biexponential decay equation with R-Square values of 0.9711 and 0.9838 for GS-AuNP and IRdye 800CW, respectively. The distribution half-lives ($t_{1/2\alpha}$) of GS-AuNP and IRdye 800CW are 5.4 ± 1.2 and 6.3 ± 2.5 min, respectively. The elimination half-lives ($t_{1/2\beta}$) of GS-AuNP and IRdye 800CW are 8.5 ± 2.1 and 0.98 ± 0.08 hr, respectively (Data presented as mean ± SD, n = 3).

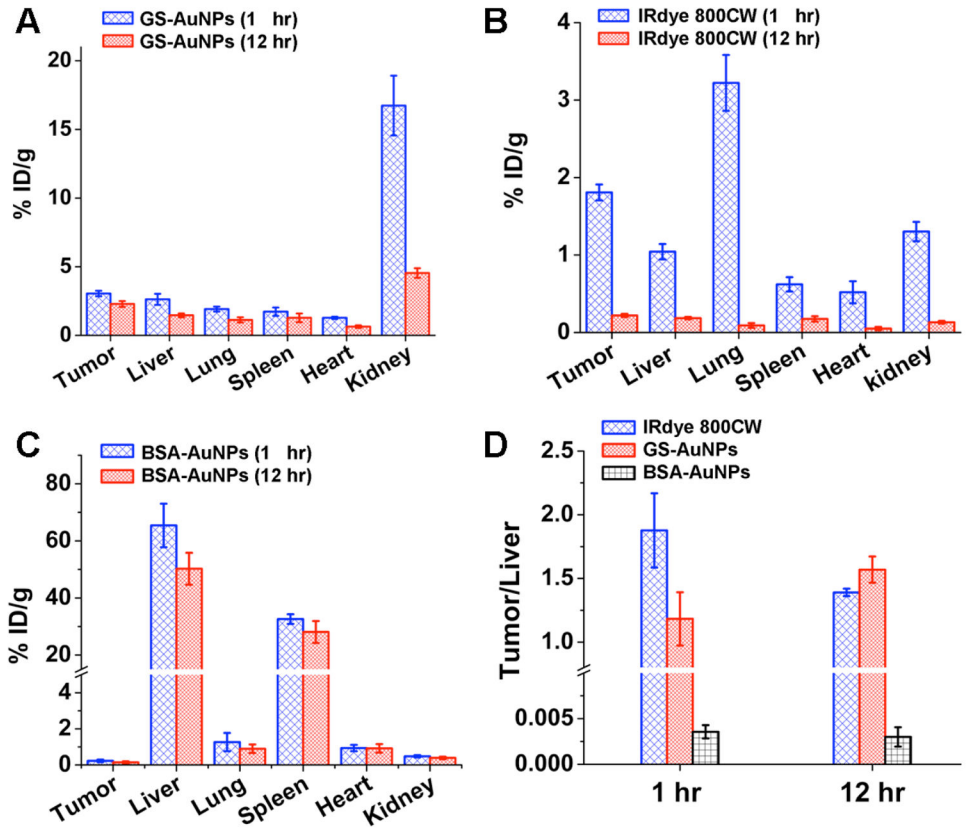

Figure 4.

Biodistribution analysis of the passive tumor targetting in MCF-7 tumor-bearing mice. The biodistributions of GS-AuNPs (A), IRdye 800CW (B), and BSA-AuNPs (C) at 1 and 12 hr p.i., respectively. D) The ratios of the probe concentration in tumor to that in liver at 1 and 12 hr p.i., respectively.